EUT Directivity and Other Uncertainty Considerations For GHz-Range Use of TEM Waveguides

Timothy E. Harrington
2701 Legacy Point Dr., Arlington, TX 76006
teharrington@aol.com

Edwin L. Bronaugh, NCE
EdB[TM] EMC Consultants
10210 Prism Dr., Austin, TX 78726
ed.bronaugh@ieee.org

Abstract: Over the past several years there has been an increasing trend to identify and minimize measurement uncertainties in most types of EMC testing. This paper describes various uncertainty influence quantities that may affect direct voltage-based or correlated E-field radiated emissions tests in most TEM waveguides, and specifically in the GTEM cell. Most TEM-waveguide emissions testing is based on the measurement of EUT total radiated power. To clarify directivity and EUT loading influences, total radiated power and field strengths measured from canonical loop antenna and slotted and raised-lid box EUTs in GTEM cells in the 30-2000 MHz frequency range is presented. Measured results from various GTEM multi-position conversion-to-free-space or -OATS schemes are compared. The intent is to describe an analysis framework and raise awareness so that operators can begin to recognize and minimize uncertainty sources, and to contribute to better understanding of correlation effects in GTEM.

INTRODUCTION

The reference test facility for EMC radiated emissions testing has traditionally been and still is the open-area-test-site (OATS). Various sizes of semi-anechoic chambers (SAC) have become a very popular but sometimes relatively expensive near equivalent to OATS. There is still interest in the EMC community for alternative test facilities, including the free-space (FS) type fully-anechoic rooms (FAR), gigahertz transverse electromagnetic (GTEM) cells and other TEM waveguides, and reverberation chambers. GTEM cells are currently used as alternative test sites for both pre- and full-compliance radiated emissions testing. A GTEM does not directly measure an OATS-equivalent field strength at a distance, but it instead measures total radiated power from an equipment-under-test (EUT). This GTEM-measured power is typically used to calculate an equivalent OATS field strength as radiated by a simple dipole. The basic GTEM correlation algorithm uses voltage readings from three orthogonal positions of an EUT to estimate total radiated power that is inserted in the usual far-field field strength formula. For some types of EUTs more positions may be necessary. Six [1], six measurement-three input (6M/3I) [2], nine [3], twelve [4], 12M/3I [5], (12+4)M/(3+1)I [6], and fifteen [7] -position one-port TEM waveguide methods have been described. These alternative correlation methods have been claimed to have advantages over the simple three-position method, thus the 6, 6M/3I, 9, 12M/3I, and 15 position methods are investigated below.

It is useful to consider testing in alternative facilities in terms of "compliance uncertainty" [8]. Compliance uncertainty encompasses the usual measurement instrumentation uncertainty, e.g., [9] for OATS testing, but also includes other effects such as EUT-to-receive-antenna mutual coupling, cable layout sensitivities, and measurement system and EUT repeatabilities. The important condition, difficult to establish other than in terms of compliance uncertainty, is whether or not testing in an alternative facility will ensure electromagnetic compatibility in the final installation of the EUT.

The empty waveguide TEM mode is defined in [2] as -0/+6 dB variation in primary E-field component over a calibration area at each frequency, and secondary (cross-polarized) components less than at least 3 dB. Similarly, an emissions correlation is defined to be valid if the average is within –0/+3 dB and the standard deviation is within 4 dB over 10 or more EUT frequencies. In practice, uncertainties may affect whether this requirement of TEM waveguide correlation results overestimating OATS can be met.

Numerous uncertainty budgets for TEM waveguide immunity tests have been previously reported, e.g., [10,11]. However, only uncertainty components that are relevant for emissions testing are described here. Limited discussions on emissions uncertainty considerations appeared in [5,12,13], and relevant factors from those papers have been included here. EUT directivity effects in alternative facilities and in EMC testing in general are presently an active research topic [e.g., 14-16]. A view of the issues related to this influence quantity is given with the test data below.

This paper has two main subjects. First a list of TEM waveguide radiated emissions testing uncertainty influence quantities is presented. Then test results using various GTEM-to-FS correlation algorithms are shown to demonstrate loading and directivity effects. Both new and a few previously published results are presented to emphasize these aspects of uncertainty. The EUTs considered are a 30cm square loop, and a 19" dummy EUT with a slot and dipole-like radiation modes. These are excited by a comb generator source with a 5 MHz line spacing [17]. The dummy EUT has been described in detail elsewhere [18-20]. Earlier data for these canonical EUTs was reported only for below 1 GHz, while here results are included for 30-2000 MHz. Finally an example GTEM radiated emissions uncertainty budget is given.

POSSIBLE RADIATED EMISSIONS UNCERTAINTY INFLUENCE QUANTITIES

Table 1 gives an extensive but maybe not exhaustive list of uncertainty influence quantities for TEM waveguide radiated emissions testing. Several of these may overlap, and may or may not make a significant difference in any particular test. It is known that OATS or SACs usually correlate to each other within about 4 dB to 8 dB [e.g., 21], therefore uncertainty components of less than 0.5 dB or so can sometimes be neglected in favor of larger issues. Under current circumstances, in the end the proof is in the correlation. At present numerical estimates for several of these components are not available, so future discussion and research may be needed. Many of these are expected to be less than 1 dB and will not be discussed.

Table 1. GTEM and TEM Waveguide Radiated Emissions Uncertainty Influence Quantities

1	Input VSWR in termination transition-frequency range
2	Input VSWR other frequencies
3	Receive cable attenuation
4	Cumulative effect of 3 times (or 6, 9, 12, 15 etc.) - voltage measurement, receiver, pre-amp uncertainties
5	Noise/comb generator uncertainties, if used in correlation
6	Use of voltage-based versus power-based tests
7	Uncertainty in GTEM-OATS correlation – Type A
8	Uncertainty in OATS reference values for correlation comparison
9	All uncertainty components from OATS test will impact agreement with GTEM predicted field strengths
10	Correct rotation positions = EUT orthogonal axes permutations
11	Alternate correlation algorithms that may vary from any reference correlation algorithm results
12	Correlation routine coding, software bugs, or formulation errors
13	Directivity value used in correlation formula
14	Difference between actual ground plane parameters versus ideal ground plane used in most correlation algorithms
15	TEM waveguide characteristic impedance at EUT location
16	Septum height variation across volume occupied by EUT
17	EUT platform, turntable, manipulator, positioner dielectric perturbation, scattering, absorption effects
18	*xyz* positioning offset (e.g., in sensitivity of 3-position correlation)
19	Field uniformity – may be analogous to OATS NSA
20	Wave impedance – may be included in field uniformity
21	Deviation from theoretical 2D asymmetric TEM cell field distribution (e_{0y})
22	Field non-planarity – may be included in field uniformity
23	Energy loss in absorber or higher-order modes
24	Cross-polar or longitudinal-mode coupling
25	Polarization mismatch
26	Change in EUT coupling for alignment parallel to floor, septum, or in between
27	EUT loading, mutual coupling, surface-current perturbations
28	Radiation pattern peak location, interception
29	EUT equivalent-dipole moments relative phase uncertainty
30	Quadrupole effects=EUT phase center location offset uncertainty
31	EUT chassis or functionality variations throughout rotations
32	Cable routing
33	Cable length
34	Cable termination

These influence quantities can be loosely categorized into effects due to the receiving system (1-4), correlation algorithm (5-14), TEM field distribution (15-24), and EUT (25-34). Discussion of any of these effects in the future can and should be done in terms of relative magnitudes in the uncertainty budget. The standard GTEM three-position electric field correlation equation is [19]

$$E_{max} = S_{max}\sqrt{30Pg} = S_{max}\frac{20k_0}{e_{0y}}\left(\frac{3g}{Z_c}\right)^{1/2}\left[10^{\frac{V_{mx}-120}{10}}+10^{\frac{V_{my}-120}{10}}+10^{\frac{V_{mz}-120}{10}}\right]^{1/2}$$

which shows that GTEM E-field is a function of EUT radiated power *P* (related to measured voltages), EUT numeric gain *g*, frequency, site geometry factor S_{max}, transmission-line impedance Z_c, and TEM mode field strength e_{0y}. The number of factors in the last square root term and the first numeric multiplier may differ among multi-position correlation methods.   An uncertainty sensitivity analysis could be done using partial derivatives of this E-field equation. In the case that correlation data is available for a particular EUT type [22], nearly all components will be included in and can be replaced by a single TEM-to-OATS/FS correlation uncertainty component. For some EUTs, directivity and relative

phase effects may be intertwined, so correlation algorithms tailored to account for either one separately may not show advantage if both effects are present.

Some of the main issues that are still under investigation fall within EUT mutual coupling, field distributions, and cable effects. A contribution on mutual coupling effects is given by the data later in this paper. Via an emissions field uniformity mapping with small dipole-like radiators, [23] shows that local cross-pol components do exist, but the effects for more realistic, larger EUTs are not described there. Reference [18] shows good correlation for various canonical EUTs, and points out that no pronounced effects are seen due to the main 130 MHz longitudinal component. Nonuniform waveguide effects [24], including higher-order modes, can have an influence on field distribution variations along the GTEM length.   These are included in the field uniformity and correlation uncertainty components.   Quadrupole effect [4,25] studies in one-port TEM waveguides have not been reported, probably because a revised correlation method would be required. Transmission between an antenna and EUT in the presence of a reflecting plane consists of primary and secondary rays, or direct and reflected. References [26,27] describe a third or tertiary ray or wave that is reflected from the EUT back to the antenna. This is a type of mutual coupling between EUT and antenna. Using an immunity-type setup, it was reported that in GTEM the tertiary wave can cause about ±3 dB response variations. However, results below with the slot- and plate-mode EUTs show less than 1 dB average variation for an EUT with size of 2/3 of the septum height.

Several standardized cable layouts, which essentially remain fixed throughout EUT rotations, are proposed in [2]. While these should provide repeatability and reproducibility advantages, results based on these setups will likely have systematic differences between each other and between the usual OATS and SAC cable layouts. These differences need more experimental investigation, after which their contributions can be included in compliance uncertainty budgets.

SUB-GHz DIRECTIVITY EFFECTS WITH EXAMPLE LOOP RADIATOR

While presently there is much discussion about directivity effects with regards to testing above 1 GHz, it is important to be aware that radiation-pattern effects can play a role in the 30-1000 MHz range as well. Although the original reference radiator concept [28] suggested the use of a 10cm loop for 200-1000 MHz site characterization., it turns out that the simple 30cm square loop is an interesting EUT for use in correlation exercises due to its complex radiation pattern shapes. An example of the possible deviations depending on initial EUT position in the GTEM is shown by the loop radiated power data in Figure 1. The start positions are shown in Figure 2. Curves 1 and 3 are low in 350 MHz vicinity, while curves 2 and 3 are low in 725 MHz vicinity. Use of the 12M/3I method [5] would give the upper envelope of the curves since the maximum is selected at each frequency. The 6M/3I method of [2] is a subset of 12M/3I, so this may not capture the peak at all frequencies, depending on EUT radiation pattern shape and symmetry.

The loop results of Figure 1 show a ripple in the response, particularly below about 600 MHz. Though bothersome, this ripple was seen to be an entirely repeatable trait of this specific comb generator unit. A same-model comb generator used in earlier tests [18,19] did not exhibit such behavior. A fourth-order
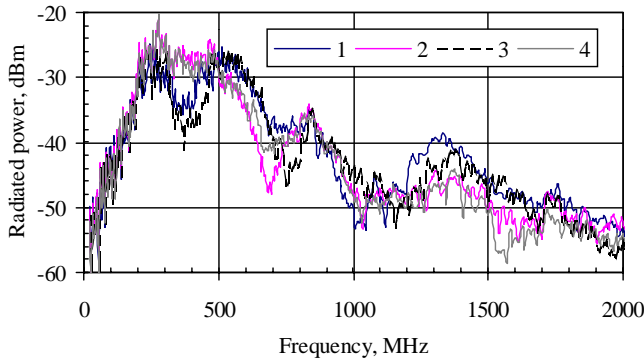
Figure 1. Loop radiated power from tests done at four start positions (times three orthogonal positions = 12 positions total) in GTEM 1750. Curve numbering order corresponds to left-to-right order in Figure 2.
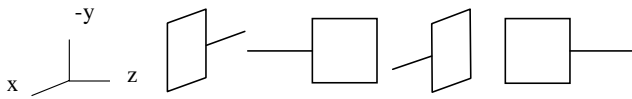

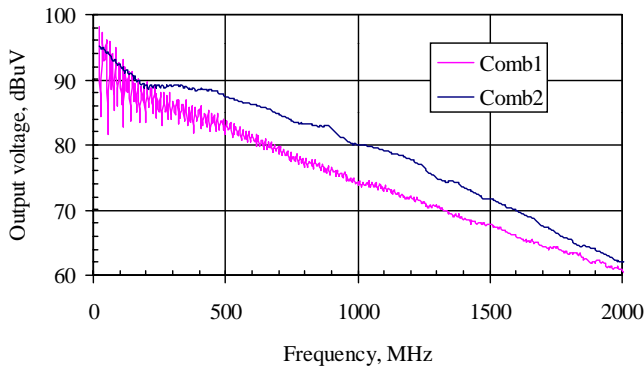**Figure 2. Schematics of loop EUT in four start positions. GTEM apex is in *x* direction and septum is in –*y* direction.**

Figure 3. Envelopes of two comb generator conducted output voltage peaks. Comb1 was used for GTEM loop tests, while Comb2 was used for FAR and box EUT test results below.

polynomial fit to the ripple curve was used to obtain differences for later use in normalizing with Comb2 test results.

Figure 4 shows a comparison of 3-, 6-, and 9-position correlated 3 m free-space field strength results A multiplier of 1 was used in the degeneracy check for the 9-position data, rather than 0.1 as suggested in [3, pg. 4]. With a 0.1 multiplier, degeneracies (singularities) in the conversion equations may not be adequately removed [29]. Deviations in the 9-position data are possibly due to dipole moment relative phase differences, as predicted in [30]. The 6-position method [1] is claimed to account for relative phase via readings at three positions at 180º from the original orthogonal positions. The 6-position results of Figure 4 indicate that the 3-position assumption of in-phase dipole moments is valid, at least for this loop EUT. The 15-position method [7] has also been presented as a way to account for dipole-moment relative phase differences. Figure 5 compares loop 3 m free-space field strength from 3- and 15-position GTEM 1750 correlations and a FAR 1-position measurement. The FAR data was normalized using the difference between the conducted output powers of Figure 3, as described above. Above 1GHz, the pattern peak occurs off boresight, so a fixed-azimuth, 1-position FAR test is insufficient,
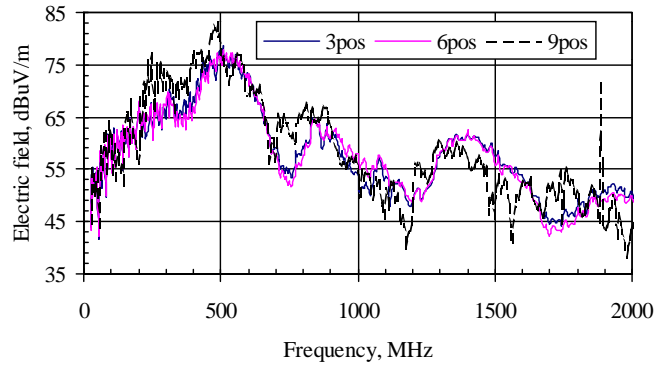

Figure 4. Comparison of loop free-space 3 m field strength from 3-, 6-, and 9-position GTEM 1750 correlations.
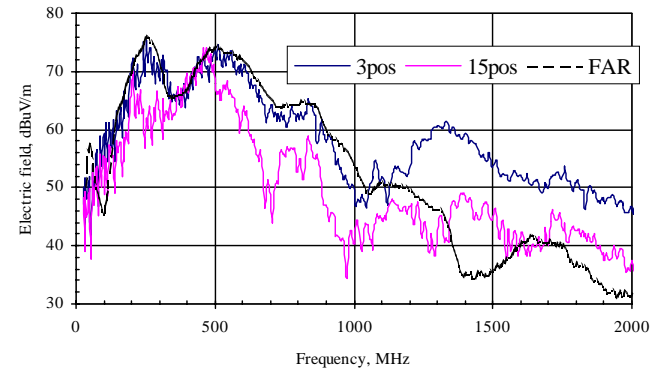

Figure 5. Loop 3 m free-space field strength from 3- and 15-position GTEM 1750 correlations compared to FAR 1-position measurement. In 150-1000 MHz, 3pos-FAR average difference is –1.8 dB, standard deviation is 2 dB.

in which case azimuth scanning in FAR may improve the correlation. Although the FAR data slightly bounds the GTEM results below 1 GHz, numerous factors can explain that, including antenna factor errors and the different receivers and comb generators used. The undulations in the FAR data below 150 MHz is suspected to be due to diminished absorber performance [18].

To better understand the decreases in the 350 and 725 MHz data of Figure 1, it is instructive to look at examples of the theoretical far-field radiation patterns of a wire square loop antenna. Figure 6 shows NEC2-calculated normalized far-field radiation patterns for 30 cm square loop. For a one-wavelength-perimeter square loop antenna, "radiation is maximum normal to the plane of the loop (along the x-axis) and in that direction is polarized parallel to the loop side containing the feed. In the plane of the loop there is a null in the direction parallel to the side containing the feed point (along the y-axis), and there is a lobe in a direction perpendicular to the side containing the feed (along the z-axis). These results are quite different from the small loop antenna which has a null on-axis and maximum (uniform) radiation in the plane of the loop" [31]. The 30cm square loop has a one-wavelength perimeter at 250 MHz, while a 10cm loop would have this resonance at about 750 MHz. In a resonant circular loop, "the current is seen to be roughly equivalent to that in a pair of parallel dipole antennas driven in phase and with a spacing approximately equal to the diameter of the loop." "The far-zone patterns for the resonant loop are also similar to those for the pair of dipoles; they have little resemblance to the figure-eight pattern of the electrically small loop" [32]. For example, nulls in the *y*-direction (90º from top of
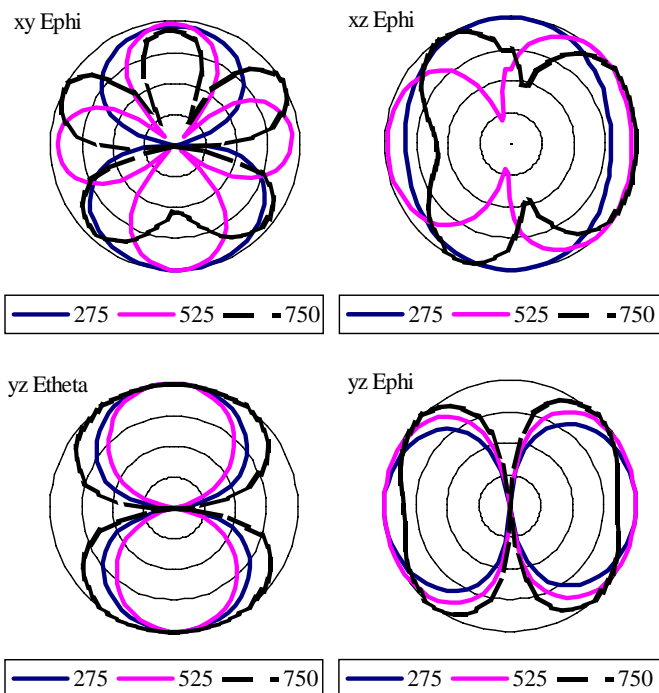
xy Ephi

xz Ephi

| —— 275 | —— 525 | – –750 |

| —— 275 | —— 525 | – –750 |

yz Etheta

yz Ephi

| —— 275 | —— 525 | – –750 |

| —— 275 | —— 525 | – –750 |

Figure 6. NEC2-calculated normalized far-field radiation patterns for 30 cm square loop. *x*-axis points up in *xy*-cut and to the right in the *xz*-cut, *z*-axis points up in *yz*-cut. Scale is 5 dB per division, -20 dB at center.

plot) of the *xy*-cut contribute to the power decrease at 750 MHz in curve 2 of Figure 1.

While an EUT gain value must be assumed when converting power measured in a reverberation chamber to field strength, in a TEM waveguide it is possible to estimate gain based on additional measurements. The $(12+4)M/(3+1)I$ [6] may be used to estimate and account for numeric directivities higher than the value of 3 assumed in the 3-position method [19]. Statistical considerations of pattern peak capture can be found in, e.g., [15].

EXAMPLE LOADING AND DIRECTIVITY EFFECTS WITH SLOTTED-BOX AND RAISED-LID EUTs

The 19U or 48 cm x 48 cm x 12 or 16 cm "simple EUT," shown in Figure 7, is a calculable and convenient EUT for use in radiated facilities comparison studies.   The raised-lid configuration simulates an equipment case with a perimeter gap, while the side-slot configuration simulates an aperture leakage.

A good comparison of Comb2/slotted box 3 m free-space field strength converted from 3-position GTEM 750 and 1750 tests is shown in Figure 8. The EUT size is equal to 0.32 times the septum height in the GTEM 1750, and 0.64 times the septum height at the EUT midpoint in the GTEM 750.   Although some individual resonances may have shifted (mutual coupling uncertainty), the overall level and shape are the same. The same GTEM 750 data is compared in Figure 9 with 15-position GTEM 750 and one-position FAR data. A free-space version of the horizontal E-field equation of [7] was used by omitting the R_2 reflected ray terms. At the time of writing, a possible discrepancy in the 15-position formulations of [7,33] was being investigated. Meanwhile, the offset seen in the 15-position data could be included as an uncertainty component. Pattern and directivity level-shift effects are important

when slotted-box type radiators are considered as an unknown radiator [19,20]. As shown in [19], a numeric gain of g=4 is a better representation for the slotted box, which if used would shift the GTEM levels in Figure 9 slightly higher.
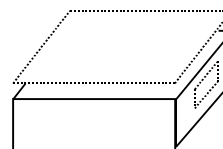

Figure 7. Schematic of box EUT. The side slot and raised lid are shown as dashed lines to indicate use in either "plate mode" or "slot mode" with a voltage source imposed, but not plate and slot modes simultaneously.

Again a good comparison of Comb2/raised-lid box 3 m free-space field strength converted from 3-position GTEM 750 and 1750 tests is shown in Figure 10. The 0º and 45º FAR data in Figure 11 show a peak emanating from the box corner near 900 MHz. Any GTEM method that does not orient the corner towards the feed may underestimate field strengths in this frequency range, since GTEM 0º and 90º start positions give near-identical readings. The 9-position method measures ±45º for each orthogonal axes permutation, so the 900 MHz-range maxima was better predicted with that method. The 9-position overestimates above 1 GHz may be due to phase errors [30] or code or formulation errors. Finally, Figure 12 shows comparison between 3- and 15-position GTEM 750 and one-position FAR data. Here all methods show relatively good agreement. Good correlation data for this EUT mode was also shown in [20].
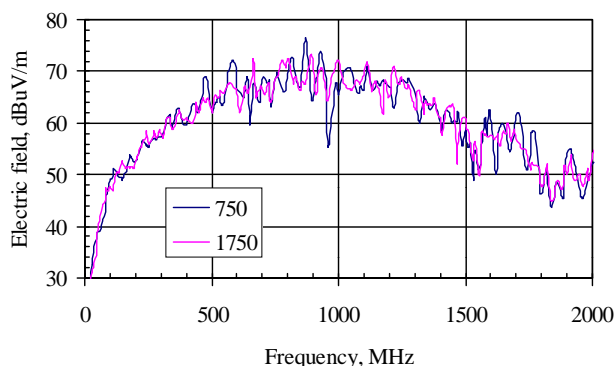

Figure 8. Slotted box EUT 3 m free-space field strength from 3-position GTEM 750 and 1750 correlations. EUT size equal to about 2/3 and 1/3 of the septum height, respectively. The average difference and standard deviation over frequency are 0.04 dB and 2.91 dB, respectively.

EXAMPLE UNCERTAINTY BUDGET FOR GTEM TEST

An example uncertainty budget is shown in Table 2 for a GTEM radiated emissions test.   Typical element values are used for a setup with spectrum analyzer, external pre-amp, cables, and GTEM. First, combined standard and expanded uncertainties are computed for the GTEM using a template like Table 2.   This GTEM contribution consists of a 4 dB field uniformity influence quantity with triangular distribution (weighting factor $1/\sqrt{6}$), and for example the correlation standard deviation σ =2.92 from Figure 9 with a normal distribution. (It is permissible to use the number of test frequencies to derive and use the standard deviation of the mean, but that will not be done in this example.) This gives an expanded uncertainty (k=2) of 4.381 dB for use as the GTEM

Table 2. Example Uncertainty Budget for Slotted-box EUT 3-position GTEM-to-FAR Correlation

| Component Source		Tolerance or σ		Max VSWR				Spec. U (k=2)			Dist.	Type Eval.	Weighting	u_s
#	Name	dB	%	In	Out	Γt	Γo	dB	%	n	(A,N,R,U)	(A, B)	Factor	dB
1	spectrum analyzer	1.049		1.5		0.2				1	N	B	1.0000	1.049
2	pre-amp			2	2.2	0.333	0.375	1.23		19	N	A	0.2294	0.141
3	GTEM				1.25		0.111	4.381		1	N	B	1.0000	2.19
4	cable1	0.277								1	R	B	0.5774	0.16
5	cable2	0.212								1	R	B	0.5774	0.123
6	comb generator ampl tol.							0.8165		1		B	0.0000	0
Mismatch Calculation		Γ1	Γ2	--				Tot. Err.			--	--	--	--
7	pre-amp : spec ana	0.375	0.2	--				0.65	--	--	U	B	0.7071	0.462
8	GTEM : pre-amp	0.111	0.333	--				0.32	--	--	U	B	0.7071	0.228
							Combined Standard Uncertainty, u(c):				N	A	--	2.495
							Expanded Uncertainty, U:				N	A	2	4.989
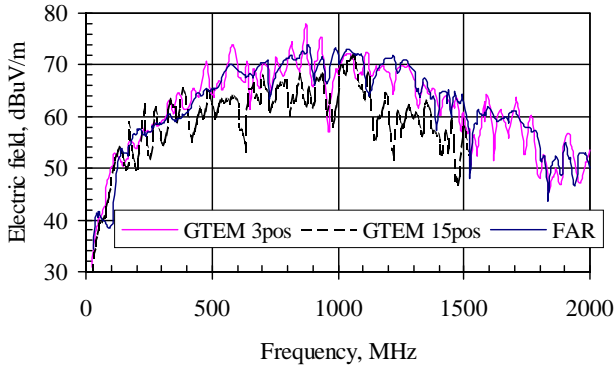
Figure 9. Slotted box 3 m free-space field strength from 3- and 15-position GTEM 750 correlations compared to FAR 1-position measurement. EUT size equal to 2/3 septum height. For 150-2000 MHz, GTEM-3-position-to-FAR average difference and standard deviation are –0.51 dB and 2.92 dB, respectively.
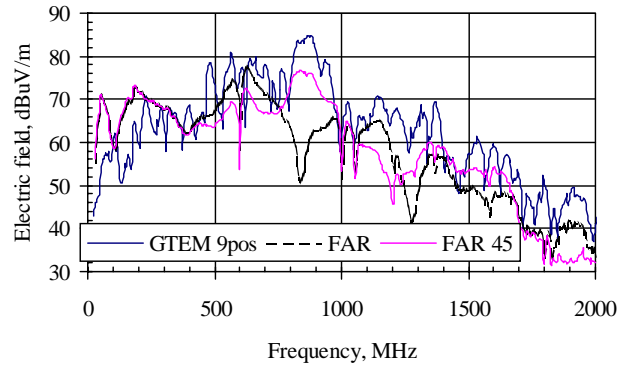

Figure 11. Raised-lid EUT 3 m free-space field strength from 9-position GTEM 750 correlation compared to two FAR azimuth position measurements at incidence normal to side and to corner (45°).
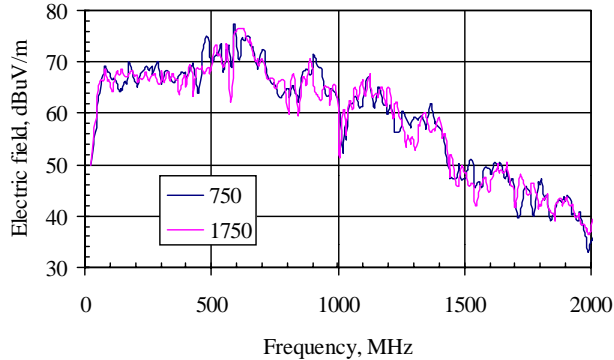

Figure 10. Raised lid EUT 3 m free-space field strength from 3-position GTEM 750 and 1750 correlations. EUT size equal to 2/3 and 1/3 septum height respectively. The average difference (1750 minus 750) and standard deviation over frequency are -0.25 dB and 2.72 dB, respectively.
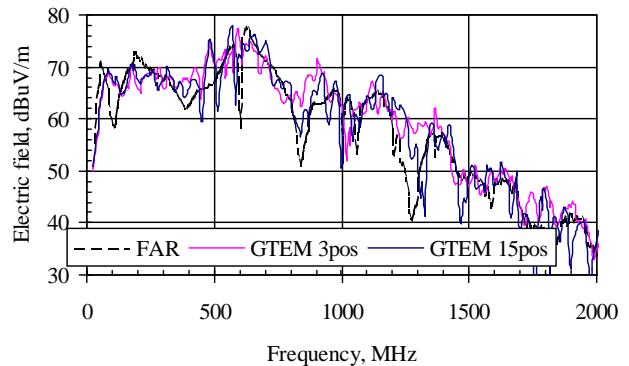

Figure 12. Raised-lid 3 m free-space field strength from 3- and 15-position GTEM 750 correlations compared to FAR 1-position measurement. 3-position-to-FAR average difference and standard deviation are 1.97 dB and 4.48 dB, respectively, in 150-2000 MHz.

component in Table 2. The final expanded uncertainty for the system is then 4.989 dB. A zero weighting factor factor is shown for the comb generator amplitude tolerance because it is included in the GTEM correlation term.

DISCUSSION AND CONCLUSIONS

Very good agreement has been shown between measured free-space and OATS radiated emissions and predictions based on simple loop and box EUT total radiated power testing inside GTEM cells. It was beyond the scope of this work to validate the 9- and 15-position

correlation methods, but the results here indicate that additional verification and experience may be needed with those methods, or at least with the software implementation versions used in this study. Rotation schemes that do not include the peak radiation lobe with matched polarization will likely give lower radiated power and converted field strengths.

Numerous uncertainty influence quantities have been summarized and reviewed. In the future, discussion of any of these effects can and should be done in terms of their magnitude relative to the total uncertainty budget magnitude. Quantities that are insignificant with respect to the combined standard uncertainty should be either ignored

or at least deprecated. Pattern, directivity, and EUT loading effects have been reviewed, but similar analyses are still needed for cable effects in TEM waveguides. In spite of the actual and perceived quirks of TEM waveguides, the experience of many GTEM users shows that GTEM works, providing good, reliable measures of the radiated emission of EM disturbances from EUTs and the immunity of EUTs to radiated EM disturbances.

REFERENCES

[1] M. Klingler, J. Rioult, J-P. Ghys, and S. Ficheux, "Wideband total radiated power measurements of electronic equipment in TEM and GTEM cells," *Intl. Zurich Symp. Electromag. Compat.*, Zurich, Switzerland, pp. 665-670, 1999.

[2] Committee Draft IEC 61000-4-20 *Electromagnetic Compatibility (EMC) – Part 4: Testing and Measurement Techniques – Section 20: Emission and Immunity Testing in Transverse Electromagnetic (TEM) Waveguides*, International Electrotechnical Commission, Geneva, Switzerland, CISPR/A/308/CD, May 2001.

[3] P. Wilson, "On correlating TEM cell and OATS emission measurements," *IEEE Trans. Electromag. Compat.*, vol. 37, no. 1, pp. 1-16, Feb. 1995.

[4] P. Wilson, D. Hansen, and D. Koenigstein, "Simulating open area test site emission measurements based on data obtained in a novel broadband TEM cell," *IEEE Natl. Symp. Electromag. Compat.*, Denver, CO, pp. 171-177, 1989.

[5] M. J. Thelberg, E. L. Bronaugh, and J. D. M Osburn, "GTEM to OATS radiated emissions correlation from 1-5 GHz," *IEEE Intl. Symp. Electromag. Compat.*, Chicago, IL, pp. 387-392, 1994.

[6] J. D. M. Osburn, "Method and apparatus for improved correlation of electromagnetic emmission [*sic*] test data," US Patent No. 5,404,098, 1992.

[7] A.-K. Lee, "An advanced correlation algorithm between GTEM and OATS for radiated emission tests," *ETRI Journal*, vol. 17, no. 3, pp. 45-63, Oct. 1995.

[8] J. J. Goedbloed, "Uncertainties in standardized EMC compliance testing," *Intl. Zurich Symp. Electromag. Compat.*, Zurich, Switzerland, Supplement, pp. 161-178, 1999.

[9] CISPR/A/291/CDV, "Accounting for measurement uncertainties when determining compliance with a limit," draft amendment to CISPR 16-3, International Electrotechnical Commission, Geneva, Switzerland, Dec. 2000.

[10] ETR 273-5 *Electromagnetic Compatibility and Radio Spectrum Matters (ERM); Improvement of radiated methods of measurement (using test sites) and evaluation of the corresponding measurement uncertainties; Part 5: Striplines*, ETSI Technical Report, European Telecommunications Standards Institute, Feb. 1998.

[11] T. M. Babij, "Evaluation of errors in the calibration of TEM cells," *Miami Technicon*, Miami, FL, pp. 199-201, 1987.

[12] M. T. Ma, "Error analysis of radiation characteristics of an unknown interference source based on power measurements," *IEEE Intl. Symp. Electromag. Compat.*, Tokyo, Japan, pp. 39-44, 1984.

[13] M. L. Crawford, and J. L. Workman, "Predicting free-space radiated emissions from electronic equipment using TEM cell and open-field site measurements," *IEEE Intl. Symp. Electromag. Compat.*, Baltimore, MD, pp. 80-85, 1980.

[14] G. Koepke, D. Hill, and J. Ladbury, "Directivity of the test device in EMC measurements," *IEEE Intl. Symp. Electromag. Compat.*, Washington, DC, pp. 535-539, 2000.

[15] G. J. Freyer, and M. G. Bäckström, "Comparison of anechoic & reverberation chamber coupling data as a function of directivity pattern," *IEEE Intl. Symp. Electromag. Compat.*, Washington, DC, pp. 615-620, 2000.

[16] P. Wilson, G. Koepke, J. Ladbury, and C. L. Holloway, "Emission and immunity standards: replacing field-at-a-distance measurements with total-radiated-power measurements," to appear in *IEEE Intl. Symp. Electromag. Compat.*, Montreal, Canada, 2001.

[17] EMCO 4630 *RefRad Reference Radiator System*, ETS, Austin, TX.

[18] T. E. Harrington, Z. Chen, and M. D. Foegelle, "GTEM radiated emissions testing and FDTD modeling," *IEEE Intl. Symp. Electromag. Compat.*, Seattle, WA, pp. 770-775, 1999.

[19] T. E. Harrington, "Total-radiated-power-based OATS-equivalent emissions testing in reverberation chambers and GTEM cells," *IEEE Intl. Symp. Electromag. Compat.*, Washington, DC, pp. 23-28, 2000.

[20] D. González Rueda, M. J. Alexander, "EUT measurement comparison between different EM environments: FAR, OATS and GTEM cell," *Intl. Zurich Symp. Electromag. Compat.*, Zurich, Switzerland, pp. 347-352, 2001.

[21] K. Hall, D. Pommerenke, and L. Kolb, "Comparison of site-to-site measurement reproducibility using UK National Physical Laboratory and Austrian Research Center test sites as a reference," *IEEE Intl. Symp. Electromag. Compat.*, Washington, DC, pp. 939-943, 2000.

[22] ANSI C63.4-2000, *Interim Standard for Methods of Measurement of Radio-Noise Emissions from Low-Voltage Electrical and Electronics Equipment in the Range of 9 kHz to 40 GHz*, The Institute of Electrical and Electronics Engineers, Inc., New York, Dec. 2000.

[23] A. Nothofer, A. C. Marvin, and J. F. Dawson, "Indirect measurement of field uniformity in TEM cells including cross-polar field components," *Intl. Zurich Symp. Electromag. Compat.*, Zurich, Switzerland, pp. 659-664, 1999.

[24] J. P. Kärst, C. Groh, and H. Garbe, "Field mode properties of loaded TEM waveguides," *Intl. Zurich Symp. Electromag. Compat.*, Zurich, Switzerland, pp. 481-486, 2001.

[25] I. Sreenivasiah, D. C. Chang, and M. T. Ma, "A critical study of emissions and susceptibility levels of electrically small objects from tests inside a TEM cell," *IEEE Intl. Symp. Electromag. Compat.*, Boulder, CO, pp. 499-507, 1981.

[26] J. Glimm, T. Shrader, K. Münter, R. Pape, M. Spitzer, "A new direct-measuring field sensor up to 1000 MHz with an analog fibre-optical link –design, traceable calibration, and results-," *Intl. Zurich Symp. Electromag. Compat.*, Zurich, Switzerland, pp. 483-487, 1999.

[27] T. Shrader, *Vergleich von Feldgeneratoren für EMV-Prüfungen* (*Comparison of Field Generators for EMC Tests*), Dr.-Ing diss., Technischen Universität Carolo-Wilhelmina zu Braunschweig, Germany, pp. 85-95, 1997.

[28] H. Garn, "A fully automatic, accurate method for the performance evaluation and calibration of absorber-lined chambers for radiated-emissions tests," *IEEE Intl. Symp. Electromag. Compat.*, Cherry Hill, NJ, pp. 19-24, 1991.

[29] A. Nothofer, *Cross-polar Coupling in GTEM Cells Used for Radiated Emission Measurements*, D. Phil. diss., Univ. York, England, 2000.

[30] L. Turnbull, and A. C. Marvin, "A treatment of the phase properties of GTEM to open-area test-site correlation techniques," *IEEE Trans. On Electromag. Compat.*, vol. 40, no. 1, pp. 62-69, Feb. 1998.

[31] W. L. Stutzman, G. A. Thiele, *Antenna Theory and Design*, New York: John Wiley & Sons, Inc., pg. 250, 1981.

[32] G. S. Smith, "Loop antennas," in *Antenna Engineering Handbook*, 3rd ed., R.C. Johnson, and H. Jasik, eds., New York: McGraw-Hill, pg. 5-13, 1993.

[33] A.-K. Lee, "An algorithm for an advanced GTEM to ground plane correlation of radiated emission test," *IEEE Intl. Symp. Electromag. Compat.*, Santa Clara, CA, pp. 58-62, 1996.